D. B. Bogy
H. J. Greenberg
F. E. Talke

Steady Solution for Circumferentially Moving Loads on Cylindrical Shells

Abstract: The steady, forced-wave solution is obtained for loads that travel with constant speed on a simply supported circular shell, the motion of which is damped externally by air. Critical speeds are identified above which the waveform, which is a standing wave in moving coordinates, exhibits shorter wavelengths in front of the load than behind it. At supercritical speeds the solution becomes unbounded, because of loss of stability, in the limit of no damping.

Introduction

Solutions for circular cylindrical shells under dynamic loading conditions of various forms have appeared in the recent literature. Payton [1] solved the problem of dynamic membrane stresses in an infinitely long elastic shell. He gave specific results for impulse-concentrated and uniform-pressure loads as well as for a circumferentially expanding pressure load. In [2] and [3], Forrestal and Alzheimer evaluated the solution derived in [1] for circumferentially moving loads. Liao and Kessel [4] considered the problem of cylindrical shells, with bending as well as membrane effects, subjected to moving loads. Their shell had finite length and was subjected to the boundary conditions of simple support. Using appropriate Fourier series decompositions in the axial and circumferential directions with a Laplace transform in time, Liao and Kessel formally derived a solution that exhibits resonant conditions at critical speeds of the moving load. For the concentrated load moving circumferentially with constant speed, their solution, Eq. (33) in [4], predicts a form that is symmetrical with respect to the moving load regardless of the speed at which the load travels. The speed-independent property is quite unexpected in view of the solution for moving loads on a simply supported plate strip given by Reismann [5], which is symmetrical for subcritical speeds but exhibits a forced-wave phenomenon for supercritical speeds with shorter wavelengths in front of the load than behind it. This phenomenon was also recently observed experimentally [6] in a short cylindrical shell having a radius-to-length ratio of three and a radius-to-thickness ratio of 1500.

The critical speed is associated with loss of stability (see [7] and [8]). The inertia enters into the steady equation in moving coordinates with an effect equivalent to compressive stress resultants and the instability is similar to that of buckling. Although the membrane solution in [1] would not be expected to have critical speeds with associated different wavelengths in front of and behind the load, the bending effects included in the shells considered in [4] should lead to such a phenomenon.

In this paper we obtain the steady, inextensible bending solution for a simply supported circular shell subjected to loads moving circumferentially at constant speeds. The analytical procedure is similar to that employed in [1]. In order to deal first with integrals that exist in the regular sense, we include external damping effects. We obtain a forced-wave solution with different wavelengths in front of and behind the load for the case of supercritical speed. The amplitudes of these waves decay exponentially with distance from the load for damped or undamped solutions at subcritical speeds, as well as for damped solutions at supercritical speeds. However, the undamped solution shows no decay at supercritical speeds—in fact, the solution obtained does not converge for this case because of the previously mentioned loss of stability.

Formulation of the problem

The geometry and loading of the shell are shown in Fig. 1. The cylinder is of length ℓ, radius a, and thickness h. The coordinates of a point are x, ϕ; the displacement components in these directions are u, v and the outward displacement is w. The loading is $q(x, \phi - Vt/a)$, which indicates that it is traveling without a change in its functional form in the circumferential direction with speed V.

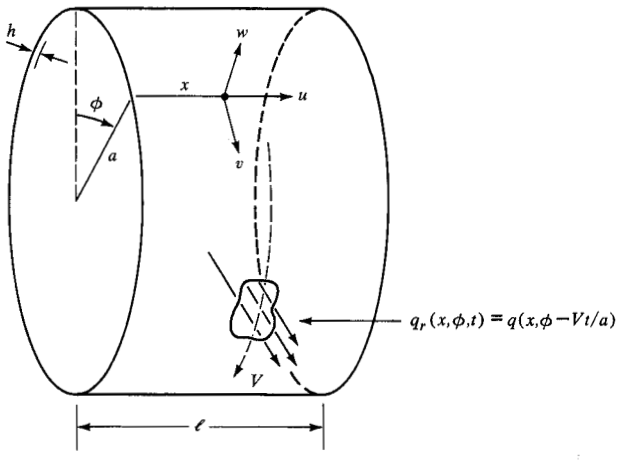

Figure 1 Geometry and loading for the cylindrical shell.

The equations used here are the thin-shell approximate equations on page 220 of Flügge [9], or page 522 of Timoshenko and Woinowsky-Krieger [10]. After using the inextensibility assumption,

$$u' = 0, \qquad u\cdot = -v', \qquad v\cdot = -w, \tag{1}$$

and adding the inertia and damping terms to the radial equation, we obtain the single equation

$$k(w'''' + 2w''\cdot\cdot + w\cdot\cdot\cdot\cdot) = \frac{-\rho h a^2}{D_1} w_{tt} - \frac{ca^2}{D_1} w_t + q\frac{a^2}{D_1}, \tag{2}$$

in which

$$k = h^2/12a^2, \quad D_1 = Eh/1-\nu^2,$$

$$(\ )\cdot \equiv \partial(\ )/\partial\phi, \quad (\ )' \equiv a\,\partial(\ )/\partial x, \tag{3}$$

where ρ, E, ν and c represent mass density, Young's Modulus, Poisson's ratio, and damping coefficient, respectively. The subscript t denotes the time derivative. The boundary conditions of simple support are

$$w = w'' = 0 \qquad \text{at } x = 0, \ell, \tag{4}$$

and because we seek a steady solution, no initial conditions are specified and the time interval is $-\infty < t < \infty$.

Steady, forced-wave solution

It is advantageous to change to dimensionless variables according to

$$\xi = x/a, \quad \tau = tV_{P_\ell}/a, \quad \hat{w} = wh/(1-\nu^2)a^2,$$

$$\hat{q} = q/E, \quad \gamma = ca/\rho h V_{Pl}, \tag{5}$$

in which the plate velocity, V_{Pl}, is given by

$$V_{Pl} = \sqrt{E/(1-\nu^2)\rho}. \tag{6}$$

Equations (2) and (4) then appear as

$$k(\hat{w}_{\xi\xi\xi\xi} + 2\hat{w}_{\xi\xi\phi\phi} + \hat{w}_{\phi\phi\phi\phi}) + \hat{w}_{\tau\tau} + \gamma\hat{w}_\tau = \hat{q} \tag{7}$$

and

$$\hat{w} = \hat{w}_{\xi\xi} = 0 \qquad \text{at} \quad \xi = 0, \ell/a, \tag{8}$$

The load $\hat{q}(\xi, \phi, \tau)$ is of steady form and moves circumferentially with constant speed V if it has the form

$$\hat{q}(\xi, \phi, \tau) = Q(\xi, \phi - (V/V_{Pl}), \tau). \tag{9}$$

To obtain the steady solution in moving coordinates for loads of this form, we set

$$\Phi = \phi - \hat{V}\tau, \quad W(\xi, \Phi) = \hat{w}(\xi, \phi, \tau), \qquad \hat{V} = V/V_{P_\ell}, \tag{10}$$

so that (7) becomes

$$k(W_{\xi\xi\xi\xi} + 2W_{\xi\xi\Phi\Phi} + W_{\Phi\Phi\Phi\Phi}) + \hat{V}^2 W_{\Phi\Phi} - \gamma\hat{V}W_\Phi = Q. \tag{11}$$

The periodicity requirements in Φ are met if we assume the form [11]

$$W(\xi, \Phi) = \sum_{n=-\infty}^{\infty} \psi(\xi, \Phi + 2n\pi). \tag{12}$$

Introducing

$$\theta = \Phi + 2n\pi, \qquad n = 0, \pm 1, \pm 2, \cdots \tag{13}$$

so that

$$-\infty < \theta < \infty \qquad \text{for} \quad -\pi < \Phi < \pi, \tag{14}$$

and defining $q(\xi, \theta)$ by

$$q(\xi, \theta) = \begin{cases} Q(\xi, \Phi) & \text{for } |\theta| \le \pi \\ 0 & \text{for } |\theta| > \pi, \end{cases} \tag{15}$$

we obtain from (11)

$$k(\psi_{\xi\xi\xi\xi} + 2\psi_{\xi\xi\theta\theta} + \psi_{\theta\theta\theta\theta}) + \hat{V}^2\psi_{\theta\theta} - \gamma\hat{V}\psi_\theta = q. \tag{16}$$

In view of the boundary conditions (8) we assume the series forms

$$\psi(\xi, \theta) = \sum_{m=1}^{\infty} \psi_m(\theta) \sin(\lambda_m \xi),$$

$$q(\xi, \theta) = \sum_{m=1}^{\infty} q_m(\theta) \sin(\lambda_m \xi), \tag{17}$$

in which

$$\lambda_m = m\pi a/\ell. \tag{18}$$

The modes $\psi_m(\theta)$ uncouple in (16) and satisfy

$$k(\lambda_m{}^4\psi_m - 2\lambda_m{}^2\psi_{m,\theta\theta} + \psi_{m,\theta\theta\theta\theta}) + \hat{V}^2\psi_{m,\theta\theta} - \gamma\hat{V}\psi_{m,\theta} = q_m. \tag{19}$$

Next we define the Fourier transform of $\psi_m(\theta)$ by

$$\bar{\psi}_m(p) = \int_{-\infty}^{\infty} \psi_m(\theta) e^{ip\theta} d\theta, \tag{20}$$

which has the inversion formula

$$\psi_m(\theta) = \frac{1}{2\pi}\int_{-\infty}^{\infty} \bar{\psi}_m(p)e^{-ip\theta}dp. \tag{21}$$

Applying the transform to (19), we obtain

$$\left[p^4 + \left(2\lambda_m{}^2 - \frac{\hat{V}^2}{k}\right)p^2 + \frac{\gamma\hat{V}}{k}ip + \lambda_m{}^4\right]\bar{\psi}_m(p) = \bar{q}_m(p)/k. \tag{22}$$

Using (22) and (21), we find

$$\psi_m(\theta) = \frac{1}{2\pi k}\int_{-\infty}^{\infty} \frac{\bar{q}_m(p)e^{-ip\theta}}{\prod_{j=1}^{4}(p - p_m{}^{(j)})}\,dp, \tag{23}$$

where $p_m{}^{(j)}$, $j = 1, 2, 3, 4$ are the four roots (for each $m = 1, 2, \cdots$) of

$$p^4 + \left(2\lambda_m{}^2 - \frac{\hat{V}^2}{k}\right)p^2 + \frac{\gamma\hat{V}}{k}ip + \lambda_m{}^4 = 0. \tag{24}$$

In view of (23), (17), and (12), the solution formally appears as

$$W(\xi, \Phi) = \sum_{n=-\infty}^{\infty}\left\{\sum_{m=1}^{\infty}\sin(\lambda_m\xi) \times\left[\frac{1}{2\pi k}\int_{-\infty}^{\infty}\frac{\bar{q}_m(p)e^{-ip\theta}}{\prod_{j=1}^{4}(p - p_m{}^{(j)})}\,dp\right]\right\}$$

$$\theta = \Phi + 2n\pi, \qquad n = 0, \pm1, \pm2, \cdots \tag{25}$$

This solution is not as formidable as it appears. For many particular choices of the load, the integral can be evaluated exactly by contour integration methods. The speed of convergence of $\Sigma_{m=1}^{\infty}$ depends on the smoothness of the assumed loading and the location of the roots $p_m{}^{(j)}$. The series $\Sigma_{n=-\infty}^{\infty}$ is such that if the $n = 0$ term becomes sufficiently small as $|\Phi|$ approaches π, as is usually the case [12], then only this term need be retained.

Properties of the solution

The solution given in (25) depends on the particular form of loading through $\bar{q}_m(p)$ and on the physical and geometrical parameters through the roots $p_m{}^{(j)}$ of (24). In order to understand this latter dependence we must study the location of these roots in the complex p plane.

Consider the transformation

$$p = i\lambda_m s, \quad \Theta_m = \frac{\hat{V}}{2\sqrt{k}\,\lambda_m}, \quad \epsilon_m = \frac{\gamma}{4\sqrt{k}\,\lambda_m{}^2}, \tag{26}$$

which carries (24) into

$$s^4 + 2(2\Theta_m{}^2 - 1)s^2 - 8\epsilon_m\Theta_m s + 1 = 0. \tag{27}$$

This is precisely Eq. (43) of [5], where a complete discussion can be found regarding the dependence of the roots $s_m{}^{(j)}$, $j = 1, 2, 3, 4$ on the reduced speed and damping parameters Θ_m, ϵ_m. If we label the $s_m{}^{(j)}$ according to

$$s_m{}^{(1)} = -a_m + ib_{1m}, \quad s_m{}^{(2)} = -a_m - ib_{1m},$$
$$s_m{}^{(3)} = a_m + ib_{2m}, \quad s_m{}^{(4)} = a_m - ib_{2m}, \tag{28}$$

then a_m is the non-negative real root of

$$a^6 + (2\Theta_m{}^2 - 1)a^4 + \Theta_m{}^2(\Theta_m{}^2 - 1)a^2 - \Theta_m{}^2\epsilon_m{}^2 = 0. \tag{29}$$

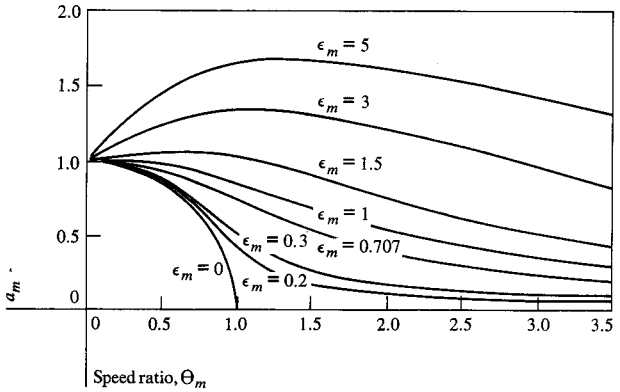

Figure 2 Solution of the characteristic equation (a_m vs Θ_m with ϵ_m as a parameter) from H. Reismann [5].

Figure 2 shows a plot of a_m as a function of Θ_m for various fixed ϵ_m. Once a_m is known, $b_{1m}{}^2$, $b_{2m}{}^2$ are computed from

$$b^2_{\binom{1}{2}m} = 2\Theta_m{}^2 - 1 + a_m{}^2 \pm 2\Theta_m\epsilon_m/a_m. \tag{30}$$

The results can be summarized as follows.

- *A. Undamped* ($\epsilon_m = 0$)
  - i) Subcritical speed ($\Theta_m < 1$)

    $b_{1m}{}^2 = b_{2m}{}^2 = 2\Theta_m{}^2 - 1 + a_m{}^2$,

    $a_m \to 1$ as $\Theta_m \to 0 \Rightarrow$ double roots at $s_m = \pm 1$
    $a_m \to 0$ as $\Theta_m \to 1 \Rightarrow$ double roots at $s_m = \pm i$
    $0 < \Theta_m < 1 \Rightarrow$ four single roots on circle $|s_m| = 1$ symmetrical about axes in s plane.
  - ii) Supercritical speed ($\Theta_m > 1$)

    $a_m = 0, \qquad b_{1m} = \pm\,[\Theta_m + \sqrt{\Theta_m{}^2 - 1}]$

    $b_{2m} = \pm\,[\Theta_m - \sqrt{\Theta_m{}^2 - 1}]$.

- *B. Damped* ($\epsilon_m \neq 0$)
  - i) Overdamped: $a_m > 0, b_{1m}{}^2 > 0, b_{2m}{}^2 < 0$.
  - ii) Underdamped: (possible only for $\epsilon_m < 1/2$)

    $a_m > 0, b_{1m}{}^2 > 0, b_{2m}{}^2 > 0$.

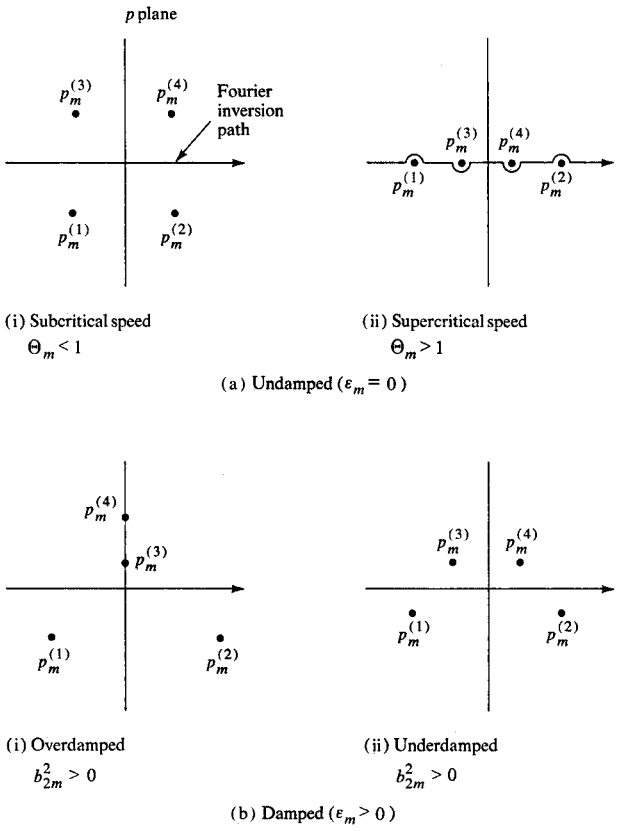

Figure 3 Root locations and integration paths in the p plane.

In view of the transformation (26) the corresponding root locations in the p plane appear as shown in Fig. 3. Also shown there are the Fourier inversion paths for the integrals in (23). Notice that in Case A(ii) the integration path is deformed around the poles of the integrand in a manner determined by considering A(ii) as the limit of B(ii) as $\epsilon_m \to 0$.

In general, all harmonics of the load function will be present in (17), so there will be a set of four poles for each $m = 1, 2, \cdots$. But when computing each $\psi_m(\theta)$ in (23) only the four poles $p_m^{(j)}$ corresponding to that mode are used. Since by (15) the range of integration for $\bar{q}_m(p)$ is at most from $-\pi < \theta < \pi$, the functions $\bar{q}_m(p)$ will introduce no singularities into the integrand in (23), so all the integrals can be evaluated by use of residue theory. To proceed further, however, it is necessary to make the load function $q(\xi, \theta)$ specific.

Line load

The simplest loading to consider is that of a line, so that $q_m(\theta)$ in (17) has the form

$$q_m(\theta) = Q_m \delta(\theta), \tag{31}$$

in which $\delta(\theta)$ is the delta function and Q_m are the Fourier sine series coefficients in (17) that depend on the functional form of the line load. For this loading

$$\bar{q}_m(p) = Q_m, \tag{32}$$

which does not depend on p.

Next we examine the solution (23) and observe that the expression $e^{-ip\theta}$ appears in the integrand, which therefore approaches zero exponentially as $|p| \to \infty$ in the upper half-plane when $\theta < 0$ and in the lower half-plane when $\theta > 0$. Application of residue theory with the appropriate closed contour yields, from (23),

$$\psi_m(\theta) = \begin{cases} i\dfrac{Q_m}{k(p_m^{(3)} - p_m^{(4)})} \times \left[\dfrac{e^{-ip_m^{(3)}\theta}}{(p_m^{(3)} - p_m^{(1)})(p_m^{(3)} - p_m^{(2)})} - \dfrac{e^{-ip_m^{(4)}\theta}}{(p_m^{(4)} - p_m^{(1)})(p_m^{(4)} - p_m^{(2)})}\right], & \theta < 0 \\ -i\dfrac{Q_m}{k(p_m^{(1)} - p_m^{(2)})} \times \left[\dfrac{e^{-ip_m^{(1)}\theta}}{(p_m^{(1)} - p_m^{(3)})(p_m^{(1)} - p_m^{(4)})} - \dfrac{e^{-ip_m^{(2)}\theta}}{(p_m^{(2)} - p_m^{(3)})(p_m^{(2)} - p_m^{(4)})}\right], & \theta > 0. \end{cases} \tag{33}$$

This expression is valid for all $m = 1, 2, \cdots$, for undamped subcritical and supercritical harmonics, as well as for overdamped and underdamped ones. The corresponding real expressions will have different forms for the various harmonic types.

For Case A(i), *undamped, subcritical* ($\epsilon_m = 0, \Theta_m < 1$) the $p_m^{(j)}$ are complex with

$$p_m^{(1)} = -p_m^{(4)}, \; p_m^{(3)} = -p_m^{(2)} = -\overline{p_m^{(4)}}$$

$$p_m^{(4)} = c_m + id_m = \lambda_m(b_{2m} + ia_m), \tag{34}$$

and (33) gives

$$\psi_m(\theta) = \begin{cases} \dfrac{Q_m e^{d_m\theta}}{4kc_m d_m(c_m^2 + d_m^2)} [c_m \cos(c_m\theta) - d_m \sin(c_m\theta)], & \theta < 0 \\ \dfrac{Q_m e^{-d_m\theta}}{4kc_m d_m(c_m^2 + d_m^2)} [c_m \cos(c_m\theta) + d_m \sin(c_m\theta)], & \theta > 0. \end{cases} \tag{35}$$

These harmonics are even functions of θ; they are oscillatory in θ with a wavelength that is inversely proportional to c_m; they decay exponentially in $|\theta|$ with constant

d_m. Since $\Theta_m \to 0$, $\epsilon_m \to 0$, and $a_m \to 1$ as $m \to \infty$, the higher harmonics decay more rapidly than do the lower ones. Such $\psi_m(\theta)$ are depicted in Fig. 4(a).

For Case A(ii), *undamped, supercritical* ($\epsilon_m = 0$, $\Theta_m > 1$) the $p_m^{(j)}$ are real with

$$p_m^{(1)} = -p_m^{(2)}, \; p_m^{(3)} = -p_m^{(4)}, \tag{36}$$

and (33) gives

$$\psi_m(\theta) = \begin{cases} \dfrac{Q_m \sin (p_m^{(4)}\theta)}{k p_m^{(4)}(p_m^{(4)} - p_m^{(2)})(p_m^{(4)} + p_m^{(2)})}, & \theta < 0 \\ \dfrac{Q_m \sin (p_m^{(2)}\theta)}{k p_m^{(2)}(p_m^{(4)} - p_m^{(2)})(p_m^{(4)} + p_m^{(2)})}, & \theta > 0. \end{cases} \tag{37}$$

Since $p_m^{(2)} > p_m^{(4)}$ these harmonics are oscillatory in θ with shorter wavelength for $\theta > 0$ [Fig. 4(b)]. They do not decay with $|\theta|$, and therefore their amplitudes at $|\theta| = \pi$ will not be diminished. This means that all values of n in (25) must be retained; and furthermore, the series cannot converge.

For Case B(i), *overdamped* ($\epsilon_m > 0$, $b_{2m}^2 < 0$) the $p_m^{(j)}$ have the forms

$$p_m^{(4)} = ik_m^{(4)}, \quad p_m^{(3)} = ik_m^{(3)}, \quad p_m^{(2)} = e_m - id_m,$$
$$p_m^{(1)} = -e_m - id_m, \quad k_m^{(3)} = d_m - |c_m|,$$
$$k_m^{(4)} = d_m + |c_m|, \quad e_m = \lambda_m b_{1m}, \tag{38}$$

with c_m, d_m defined in (34). Equation (33) yields for these roots

$$\psi_m(\theta) = \begin{cases} \dfrac{Q_m}{k(k_m^{(4)} - k_m^{(3)})}\left[\dfrac{e^{k_m^{(3)}\theta}}{e_m^2 + (k_m^{(3)} + d_m)^2} - \dfrac{e^{k_m^{(4)}\theta}}{e_m^2 + (k_m^{(4)} + d_m)^2}\right], & \theta < 0 \\ \dfrac{Q_m e^{-d_m\theta}}{k e_m[(-|c_m|^2 - e_m^2 + 4d_m^2)^2 + 16 e_m^2 d_m^2]} \\ \quad \times [4e_m d_m \cos (e_m\theta) + (-|c_m|^2 - e_m^2 + 4d_m^2) \sin (e_m\theta)], & \theta > 0. \end{cases} \tag{39}$$

Since $d_m > |c_m|$ it follows that both $k_m^{(3)}$, $k_m^{(4)}$ are positive, so these harmonics are non-oscillatory and decay exponentially in $|\theta|$ for $\theta < 0$. For $\theta > 0$ they are oscillatory, with wavelength proportional to e_m^{-1} and they decay exponentially in θ with constant d_m [see Fig. 4(c)].

Finally, for Case B(ii), *underdamped* ($\epsilon_m > 0$, $b_{2m}^2 > 0$), the $p_m^{(j)}$ have the forms

$$p_m^{(4)} = c_m + id_m, \quad p_m^{(3)} = -c_m + id_m,$$
$$p_m^{(2)} = e_m - id_m, \quad p_m^{(1)} = -e_m - id_m,$$

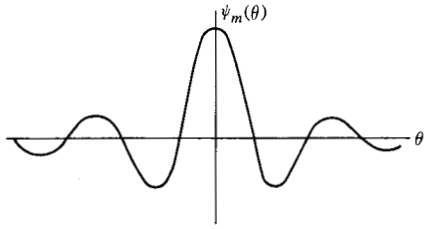

(a) A (i) Undamped subcritical modes

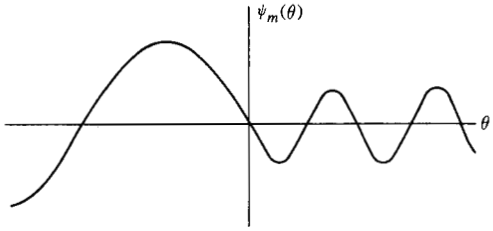

(b) A (ii) Undamped supercritical modes

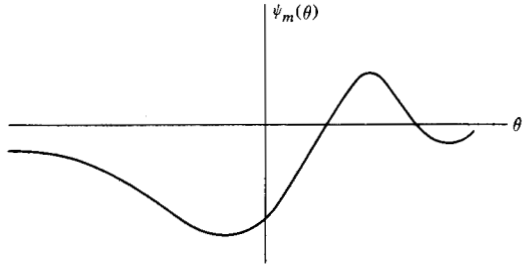

(c) B (i) Overdamped modes

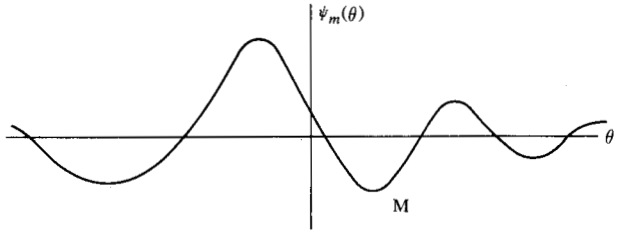

(d) B (ii) Underdamped modes

Figure 4 Form of modes for the different root locations in Figure 3.

$$(c_m, d_m, e_m) = \lambda_m(b_{2m}, a_m, b_{1m}), \tag{40}$$

and (33) yields

$$\psi_m(\theta) = \begin{cases} \dfrac{Q_m e^{d_m\theta}}{k c_m[(e_m^2 - c_m^2 + 4d_m^2)^2 + 16 c_m^2 d_m^2]} \\ \quad \times [4c_m d_m \cos (c_m\theta) - (e_m^2 - c_m^2 + 4d_m^2) \sin (c_m\theta)], & \theta < 0 \\ \dfrac{Q_m e^{-d_m\theta}}{k e_m[(c_m^2 - e_m^2 + 4d_m^2)^2 + 16 e_m^2 d_m^2]} \\ \quad \times [4e_m d_m \cos (e_m\theta) + (c_m^2 - e_m^2 + 4d_m^2) \sin (e_m\theta)], & \theta > 0. \end{cases} \tag{41}$$

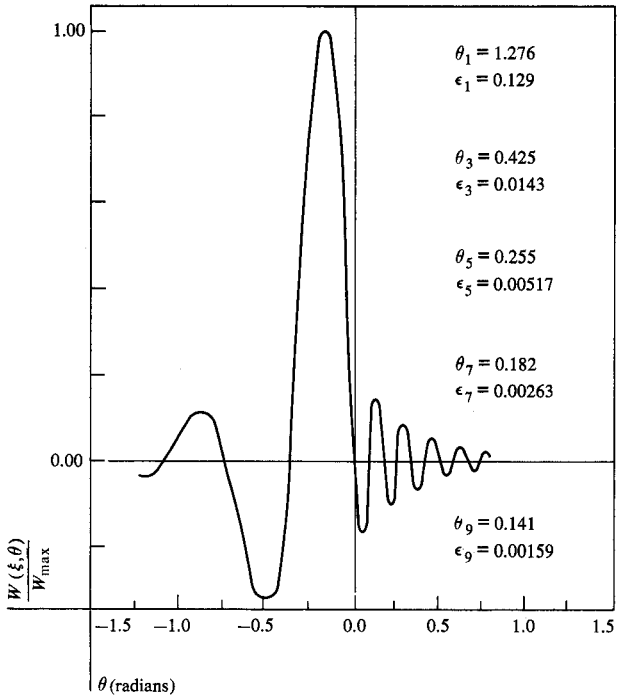

Figure 5 Steady solution in the center of the cylinder ($\xi = \ell/2a$) due to a circumferentially moving load (see text). Parameters are $V = 15.24$ m/s (600 in/s), $c = 8.896 \times 10^{-5}$ N (2×10^{-4} lb/in.-s), $a = 3.81$ cm (1.5 in.), and $\ell = 0.635$ cm (0.25 in.). Odd mode values of Θ_m and ϵ_m show that each mode is underdamped.

These harmonics are oscillatory in θ and, because $e_m > c_m$, the wavelength for $\theta > 0$ is shorter than for $\theta < 0$. The oscillations are damped exponentially in $|\theta|$ with the same constant for $\theta > 0$ and $\theta < 0$ [Fig. 4(d)].

A numerical example for the steady wave solution due to a circumferentially moving line load is shown in Fig. 5. In this example the first nine modes in Eq. (25) have been used to calculate the normalized deflection in the center of the shell. The reduced speed and damping parameters θ_m and ϵ_m are shown for the odd modes and indicate that each of the modes is underdamped. The even modes are absent because the loading is symmetric.

Discussion and conclusions

The steady forced-wave solution derived here for circumferentially moving loads clearly exhibits the phenomenon of critical speeds, above which the standing waveform (in moving coordinates) in front of the load has a shorter wavelength than that behind it. We find, however, that such a steady solution for supercritical speeds does not converge in the absence of damping. This is so because the $\psi_m(\theta)$ do not decay as $|\theta| \to \infty$, so that the series $\Sigma_{n=-\infty}^{\infty}$ does not converge, a result of the dynamic stability loss of the type discussed in [7] and [8].

We note that the path of integration for the Case A(ii) as shown in Fig. 3 is deformed around the poles in a manner dictated by considering Case B(ii) in the limit as damping vanishes. If the damping had originally been neglected altogether, the proper path for A(ii) would not have been known *a priori*, i.e., radiation conditions in moving coordinates would have to be applied to determine it; yet different paths lead to quite different results. In particular, if the path were deformed under the two poles on the negative real axis and over those on the positive real axis, or if the path were taken straight through all the poles on the real axis, then a symmetrical form would result for the subcritical and supercritical cases.

References and notes

1. R. G. Payton, "Dynamic Membrane Stresses in a Circular Elastic Shell," *J Appl. Mech.* **28,** 417 (1961).
2. M. J. Forrestal and W. E. Alzheimer, "Dynamic Response of a Circular Elastic Shell to Circumferentially Moving Forces," *AIAA Journal* **6,** No. 11, 2231 (1968).
3. M. J. Forrestal and W. E. Alzheimer, "Response of a Circular Elastic Shell to Moving and Simultaneous Loads," *AIAA Journal* **8,** No. 5, 970 (1970).
4. E. N. K. Liao and P. G. Kessel, "Response of Pressurized Cylindrical Shells Subjected to Moving Loads," *J Appl. Mech.* **39,** 227 (1972).
5. H. Reismann, "Dynamic Response of an Elastic Plate Strip to a Moving Line Load," *AIAA Journal* **1,** No. 2, 354 (1963).
6. F. E. Talke and R. C. Tseng, IBM Research Laboratory, San Jose, California; experimental results to be published.
7. A Jahanshahi and J. Dundurs, "Concentrated Forces on Compressed Plates and Related Problems for Moving Loads," *J. Appl. Mech.* **31,** *Trans. ASME* **88,** Series E, 1, 83 (1964).
8. K. Piszczek, "The Possibility of Dynamic Stability Loss Under Moving Concentrated Loads," *Archivum Mechaniki Stosowanij* **10,** 195 (1958).
9. W. Flügge, *Stresses in Shells*, Springer-Verlag, New York, 1960.
10. S. Timoshenko and W. Woinowsky-Krieger, *Theory of Plates and Shells*, McGraw-Hill Book Co., Inc., New York, 1959.
11. See [1] and references given there for a discussion regarding the use of such a form to satisfy periodicity requirements.
12. We will see, however, that this is *not* the case for the undamped solution at sufficiently large speeds.

Received December 27, 1973

Dr. Bogy is located at the Department of Applied Mechanics, University of California at Berkeley. Dr. Greenberg and Dr. Talke are located at the IBM Research Division Laboratory, Monterey and Cottle Roads, San Jose, California 95193.